PAPER

NJC www.rsc.org/njc

Anion binding by Ag(I) complexes of urea-substituted pyridyl ligands

David R. Turner,[a] Benjamin Smith,[a] Elinor C. Spencer,[a] Andres E. Goeta,[a] Ivana Radosavljevic Evans,[a] Derek A. Tocher,[b] Judith A. K. Howard[a] and Jonathan W. Steed*[a]

[a] *Department of Chemistry, University of Durham, South Road, Durham, UK DH1 3LE. E-mail: jon.steed@durham.ac.uk; Fax: +44 (0)191 384 4737; Tel: +44 (0)191 334 2085*

[b] *Department of Chemistry, University College London, 20 Gordon Street, London, UK WC1H 0AJ*

Received (in Montpellier, France) 12th October 2004, Accepted 10th November 2004
First published as an Advance Article on the web 9th December 2004

A series of Ag(I) complexes of ureidopyridyl ligands **1** and **2** have been prepared from oxo-anion salts. In all cases the new materials contain the AgL_2^+ cation interacting with oxo-anions *via* the urea moiety. The complexes containing the *para* ligand **2**: $[Ag(\mathbf{2})_2]CF_3SO_3 \cdot 2H_2O$ (**3**), $[Ag(\mathbf{2})_2]CH_3CO_2 \cdot 1.33H_2O \cdot MeOH$ (**4**) and $[Ag(\mathbf{2})_2]NO_3 \cdot H_2O$ (**5**), all exhibit remarkably similar chain-like structures based around a linear Ag(I) centre, despite the change in the counter-ion. A recurring $R_2^2(8)$ hydrogen-bonding ring motif between the urea group and the oxo-anion is observed in almost all cases. An exception to this trend is the anhydrous nitrate structure $[Ag(\mathbf{2})]NO_3$ (**6**) in which the nitrate is coordinated in a bridging position between two silver centres, which adopt distorted trigonal pyramidal geometries. Structures containing the ligand **1**, $[Ag(\mathbf{1})_2]CF_3SO_3 \cdot 0.5H_2O$ (**7**), $[Ag(\mathbf{1})_2]CF_3SO_3 \cdot H_2O \cdot MeCN$ (**8**), $[Ag(\mathbf{1})_2]_2SO_4$ (**9**), $[Ag(\mathbf{1})_2]NO_3 \cdot MeOH$ (**10**) and $[Ag(\mathbf{1})_2]NO_3 \cdot 0.5MeOH \cdot 0.5MeNO_2$ (**11**), display very different geometries, although the $R_2^2(8)$ is observed to persist throughout. The most notable of these structures are **10** and **11** in which the nitrate anion is chelated within a 'pincer' arrangement by the silver complex. The nitrate anion is situated asymmetrically within the cavity of the host complex. This discrete nitrate complex persists in solution with strong nitrate binding by the $[Ag(\mathbf{1})_2]^+$ host compared to other anions being observed.

Introduction

The binding and detection of anionic species by synthetic receptors is currently an area of significant interest.[1–3] The intrinsic challenges of anion binding, compared to cationic or neutral guests, is compensated for by the relevance and benefits of such systems in biological[4] and environmental sensing[5] applications. Although the majority of anion receptors have been based around organic scaffolds, there has been a recent and growing trend towards the use of metal-based assemblies as host species. Hosts assembled around metal centres can be either inert or covalent entities[6] or can themselves be formed under thermodynamic control in solution.[7–10] Labile host systems can be advantageous, in that the presence of certain guest species may template the formation of the host and stabilise the self-assembled complex.

We now present a simple, self-assembling host based around a urea-substituted pyridyl ligand that shows remarkable shape selectivity for nitrate in the solid state and in solution. We contrast this discrete species with a variety of extended hydrogen-bonded polymers linked *via* host···anion interactions. Part of this work has previously been communicated.[11]

Results and discussion

Extended hydrogen-bonded systems

We have previously reported the ureidopyridyl ligands **1** and **2** in the context of solid-state networks involving hydrogen bonds to metal-bound chloride.[12] The ligand **2** has also been used within systems displaying marked metal distortion due to the strength of multiple hydrogen bonds.[13] Urea is well-known in its ability to interact well with oxo-anions as such a pairing offers the possibility of forming an $R_2^2(8)$ hydrogen-bonded ring (Fig. 1).[10,14,15] A search of the Cambridge Structural Database (CSD)[16] reveals many structures involving urea in this type of interaction with a variety of oxo-anions. The $R_2^2(8)$ geometry of the interaction is expected from Etter's rules since the urea group and the oxo-anions represent, respectively, the strongest hydrogen-bond donors and acceptors in the crystal.[17] It is therefore expected that the combination of Ag(I) salts with **1** and **2** would produce systems in which the complex-anion interaction occurs *via* such a motif.

Ligands **1** and **2** were reacted with $AgNO_3$, $AgCF_3SO_3$, $AgCH_3CO_2$ and Ag_2SO_4, resulting in seven new materials. Four species (Table 1) were obtained using ligand **2**, namely $[Ag(\mathbf{2})_2]CF_3SO_3 \cdot 2H_2O$ (**3**), $[Ag(\mathbf{2})_2]CH_3CO_2 \cdot 1.33H_2O \cdot MeOH$ (**4**), $[Ag(\mathbf{2})_2]NO_3 \cdot H_2O$ (**5**) and $[Ag(\mathbf{2})_2]NO_3$ (**6**). The new compounds were characterised by X-ray crystallography while bulk composition was confirmed by elemental analysis. The crystal structures of **3–5** all contain the $[Ag(\mathbf{2})_2]^+$ cation, which adopts an essentially linear coordination geometry around the Ag(I) centre. The N–Ag–N angle is slightly removed from 180° in all cases with the exact deviation dependant upon the proximity of other potentially ligating solvent groups. The linear geometry of the cationic complex gives rise to chain-like motifs running through these three structures.

The structure of **3** involves a triflate anion interacting with one of the urea groups *via* two of the sulfonate oxygen atoms in an $R_2^2(8)$ motif (Fig. 2). The third oxygen atom receives a hydrogen bond from one of the two enclathrated water molecules within the structure. This water molecule itself receives hydrogen bonds from the remaining urea group in an $R_1^2(6)$ motif. The second water molecule is weakly coordinated to the silver centre, resulting in a distortion from linearity of the

DOI: 10.1039/b415818k

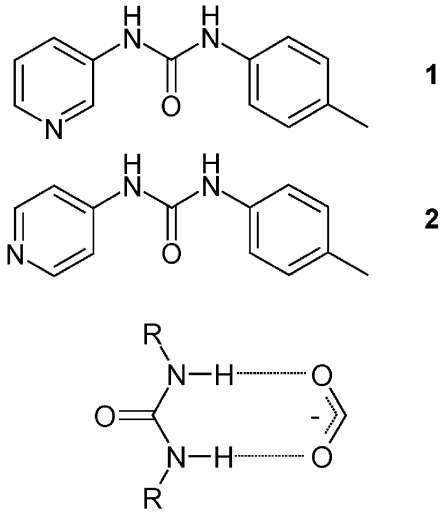

Fig. 1 The $R_2^2(8)$ hydrogen bond motif that can form between urea and an oxo-anion.

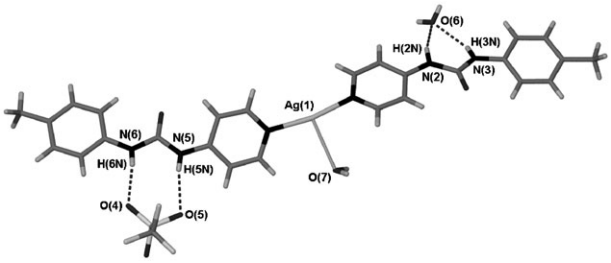

Fig. 2 The immediate environment around one $[Ag(\mathbf{2})_2]^+$ complex in the structure of **3** with a weak silver-oxygen interaction, Ag(1)–O(7), of 2.685(4) Å. Hydrogen bond data are shown in Table 2.

N–Ag–N axis, with an angle of 168.7(2)°. This solvent molecule also bridges two urea oxygen atoms in neighbouring molecules (Fig. 3). The sheets of $[Ag(\mathbf{2})_2]^+$ in the structure are stacked above each other through multiple face-to-face π-π interactions.

The acetate containing structure, **4**, closely resembles that of **3**, with the acetate anion residing in the same position as occupied by the triflate (Fig. 4). The remaining urea site is once more occupied by an enclathrated water molecule. Methanol is also included within the structure and engages in a weak interaction with the Ag(I) centre [Ag–O, 2.621(2) Å], again causing a distortion from a linear coordination geometry, with an N–Ag–N angle of 168.1(1)°. There is also a partial occupancy water molecule enclathrated within the asymmetric unit. As with the triflate complex, the cationic complexes are π-stacked with the enclathrated water occupying a bridging position between neighbouring molecules and also hydrogen bonding to the acetate anions. The methanol is also involved in hydrogen-bond donation to the acetate.

The structure of $[Ag(\mathbf{2})_2]^+$ in the nitrate complex **5** has the same general form as complexes **3** and **4** and consists of a linear $Ag(\mathbf{2})_2^+$ cation binding the anion to one urea group in an $R_2^2(8)$ motif. Differences arise in the nature of the enclathrated solvent in the structure. No interaction between the solvent and the silver centre is observed. Instead, the solvent occupies a position where it bridges urea protons of one molecule and a urea carbonyl oxygen on another. The water molecule also interacts with the nitrate anion forming an $R_3^3(10)$ pattern (Fig. 5).

A second nitrate structure was also obtained, complex **6**, which does not have any solvent enclathrated within it and which adopts a 1 : 1 Ag : **2** stoichiometry. The only difference between the formation conditions of these two materials was the solvent used: acetonitrile and methanol for **5** and **6**, respectively. The structure of complex **6** is radically different to that of the hydrated 1 : 2 structure. Rather than the more common linear geometry the Ag(I) centre exists in a distorted trigonal geometry coordinated to one pyridyl and two nitrato ligands.[18] This unit forms a silver–nitrate–silver coordination polymer (Fig. 6). The polymeric chains are connected together *via* urea···nitrate hydrogen bonding with the $R_2^2(8)$ motif that is so prevalent within this series of structures (Fig. 7). The structure of **6** has the nitrate positioned in the correct geometry to form a bidentate interaction but at a long Ag–O distance of 2.739(6) Å. A number of other silver nitrate coordination polymers are known with nitrate adopting both bidentate and monodentate coordination modes.[19,20]

The *para* substitution of the urea upon the pyridyl ring in **2** allows for chain-like architectures to form readily within Ag(I) complexes of this ligand, as seen in **3–5**. However, when the urea group is situated in the *meta* position, as in ligand **1**, very different structures, both from those discussed above and from each other, are observed (Table 3), although crucially, the urea···anion $R_2^2(8)$ motif is retained in all but one of the structures (that of **8**). The structure of the triflate complex $[Ag(\mathbf{1})_2]CF_3SO_3 \cdot 0.5H_2O$ (**7**) is the most akin to those formed using **2** and displays a geometry in which the ligands are rotated 180° away from each other around a linearly

Table 1 Crystallographic data for complexes **3–6**

	3	**4**	**5**	**6**
Formula	$C_{27}H_{30}AgF_3N_6O_7S_1$	$C_{29}H_{35}AgN_6O_{6.25}$	$C_{26}H_{28}AgN_7O_6$	$C_{13}H_{13}AgN_4O_4$
M	747.50	676.86	642.42	397.14
Crystal system	Triclinic	Triclinic	Monoclinic	Monoclinic
Space group	P-1	P-1	$C2/c$	$P2_1/c$
a/Å	10.2106(9)	9.3295(5)	38.1880(16)	7.0590(14)
b/Å	11.4626(11)	12.9275(6)	10.1919(4)	8.5990(17)
c/Å	14.2081(14)	13.1198(6)	13.7940(5)	22.610(5)
α/°	72.229(2)	83.850(2)	90	90
β/°	89.484(2)	76.896(2)	98.755(3)	94.14(3)
γ/°	69.943(2)	75.806(2)	90	90
U/Å^3	1479.0(2)	1491.86(13)	5306.2(4)	1368.9(5)
Z	2	2	8	4
μ/mm^{-1}	0.828	0.729	0.815	1.498
Unique reflections	4253	6807	3801	3113
Observed reflections	3181	5592	3436	2160
R_{int}	0.0688	0.0365	0.0201	0.1085
wR_2 (all data)	0.0814	0.0950	0.0686	0.1814
R [$I \geq 2\sigma(I)$]	0.0403	0.0419	0.0316	0.0800

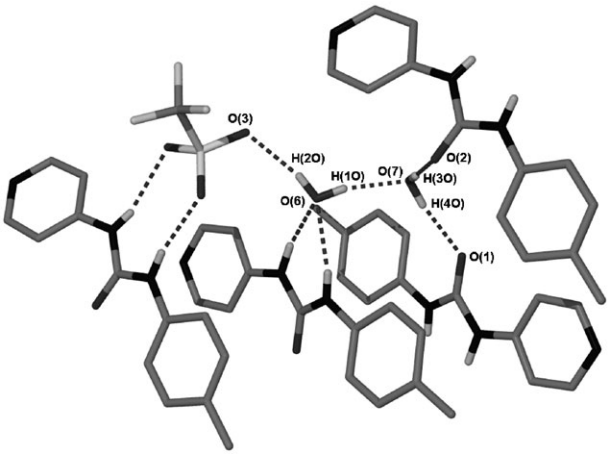

Fig. 3 Hydrogen bonding involving enclathrated water within the structure of **3**. Some ligands are omitted for clarity. Hydrogen bond data are shown in Table 2.

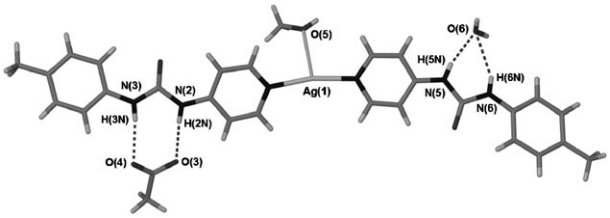

Fig. 4 The immediate environment around one $[Ag(\mathbf{2})_2]^+$ unit in the structure of **4** with a weak silver-methanol interaction, Ag(1)–O(5), of 2.621(2) Å. Hydrogen bond data are shown in Table 2.

coordinated silver atom, with the urea protons facing away from the metal centre (Fig. 8). The triflate anions bridge urea groups, once more forming both $R_2^2(8)$ and $R_1^2(6)$ rings. All of the urea groups are therefore involved in hydrogen bonding with triflate anions. The sulfonate group is disordered between these two ring-forming positions. The long-range structure is composed of discrete, helical trimers that are held together by Ag–O and CH···O interactions (Fig. 9).

A second triflate structure was obtained in which both water and acetonitrile are enclathrated: $[Ag(\mathbf{1})_2]CF_3SO_3 \cdot H_2O \cdot MeCN$ (**8**), in the chiral space group $P2_1$. This difference in the enclathrated solvent, brought about due to different reaction conditions, results in a different conformation of the $Ag(\mathbf{1})_2^+$ cation and therefore very different intermolecular interactions from those in the structure of **7**. Whereas in the structure of **7** the urea NH groups are facing away from the central silver atom, the structure of **8** has these groups facing inwards, although the arms are still rotated 180° away from each other about the N–Ag–N axis (Fig. 10). The triflate anion within **8** shows no disorder, arising from the fact that it is held in place by six hydrogen bonds, with each oxygen atom receiving two. The donor groups are a urea group, with the recurring $R_1^2(6)$ motif, one hydrogen bond from the enclathrated water (which is involved in a bridging position with a urea oxygen atom) and three pyridyl CH···O interactions (Fig. 11). This arrangement makes the triflate anion hydrogen-bond saturated.

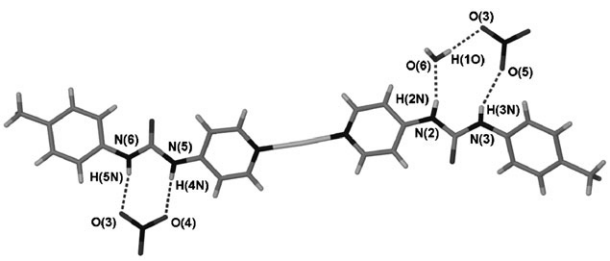

Fig. 5 The environment around one $[Ag(\mathbf{2})_2]^+$ unit in **5**. Hydrogen bond data are shown in Table 2.

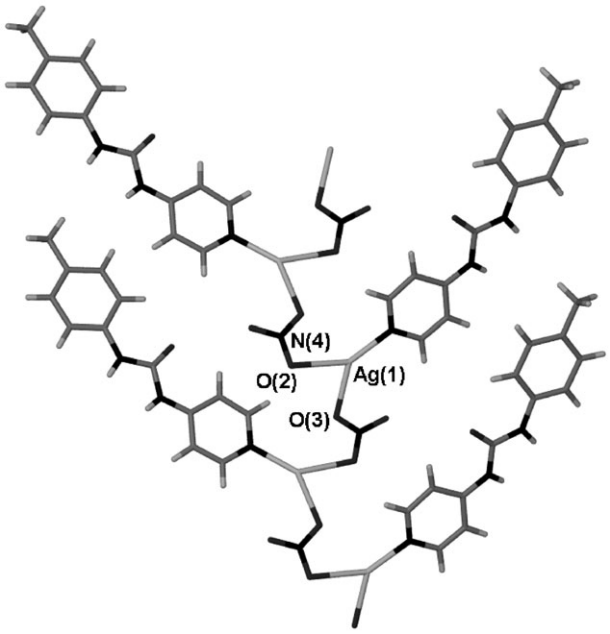

Fig. 6 A silver-nitrate coordination polymer running through the structure of **6**. Selected distances (Å): Ag(1)–O(2), 2.510(6); Ag(1)–O(3), 2.334(7).

The sulfate complex $[Ag(\mathbf{1})_2]_2SO_4$ (**9**) forms helical, interdigitating stacks in the solid-state structure (Fig. 12). These chains are held together by virtue of long-range Ag–O interactions [3.217(2) Å] utilising the urea oxygen atom. The sulfate anion, as in the previous structures, is bound to the urea protons in an $R_2^2(8)$ motif on the 'outside' of the complex. Each sulfate anion is surrounded by four urea donors, making the oxygen atoms hydrogen-bond saturated. The structure bears a close resemblance to previous sulfate-containing structures using the same ligand coordinated to octahedral metal centres.[13]

Discrete structures

The most interesting complexes from an anion binding standpoint, however, are those containing the $[Ag(\mathbf{1})_2]NO_3$ complex. Two solvates of this complex were obtained, $[Ag(\mathbf{1})_2(MeOH)]NO_3$ (**10**), and a co-crystal, $2[Ag(\mathbf{1})_2(MeOH)]NO_3 \cdot 3[Ag(\mathbf{1})_2(MeNO_2)]NO_3$ (**11**). Unlike the other structures reported in this work, the urea hydrogen atoms are orientated 'inwards'

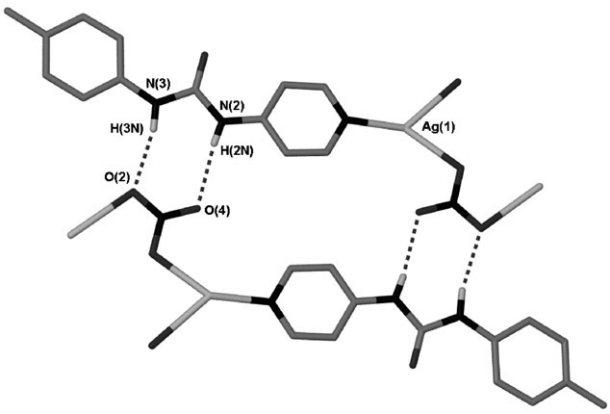

Fig. 7 Hydrogen bonding between coordination polymer chains in **6**. Hydrogen bond data is given in Table 2.

Table 2 Hydrogen bond data for structures **3–6**

	Symmetry equivalent	d(D–H)/Å	d(H···A)/Å	d(D···A)/Å	∠(D–H···A)/°
Complex **3**					
N(2)–H(2N)···O(6)	x, y, z	0.91(5)	1.94(5)	2.814(6)	162(4)
N(3)–H(3N)···O(6)	x, y, z	0.78(4)	2.22(4)	2.937(6)	153(4)
N(5)–H(5N)···O(5)	x, y, z	0.74(4)	2.27(4)	2.992(5)	163(4)
N(6)–H(6N)···O(4)	x, y, z	0.83(5)	2.11(5)	2.927(5)	169(4)
O(7)–H(4O)···O(1)	$-x, -y + 1, -z$	0.81(5)	1.94(5)	2.747(5)	172(5)
O(7)–H(3O)···O(2)	$-x, -y, -z + 1$	0.92(9)	1.82(9)	2.735(5)	171(8)
O(6)–H(2O)···O(3)	$-x, -y, -z + 1$	0.82(6)	2.10(6)	2.878(5)	159(6)
O(6)–H(1O)···O(7)	$x, y + 1, z$	0.82(7)	1.91(7)	2.713(5)	167(7)
Complex **4**					
N(2)–H(2N)···O(3)	x, y, z	0.78(4)	2.05(4)	2.826(3)	173(4)
N(3)–H(3N)···O(4)	x, y, z	0.78(3)	2.11(3)	2.888(3)	173(3)
N(5)–H(5N)···O(6)	x, y, z	0.79(4)	2.12(4)	2.889(3)	163(3)
N(6)–H(6N)···O(6)	x, y, z	0.77(3)	2.40(3)	3.109(4)	154(3)
O(5)–H(1O)···O(4)	$x, y, z - 1$	0.77(4)	1.99(5)	2.747(3)	166(5)
O(6)–H(2O)···O(3)	$-x + 2, -y + 1, -z$	0.795(10)	2.10(2)	2.878(4)	164(6)
O(6)–H(3O)···O(1)	$-x + 1, -y + 1, -z$	0.75(5)	2.12(6)	2.841(3)	164(6)
Complex **5**					
N(2)–H(2N)···O(6)	x, y, z	0.79(4)	2.06(4)	2.838(4)	165(3)
N(3)–H(3N)···O(5)	$x + 1/2, y - 1/2, z$	0.73(4)	2.33(4)	2.977(4)	148(4)
N(5)–H(5N)···O(4)	x, y, z	0.78(3)	2.17(4)	2.950(4)	174(4)
N(6)–H(6N)···O(3)	x, y, z	0.77(3)	2.18(3)	2.926(4)	163(3)
O(6)–H(1O)···O(3)	$x + 1/2, y - 1/2, z$	0.76(4)	2.04(5)	2.792(4)	173(5)
O(6)–H(2O)···O(1)	$x, -y, z - 1/2$	0.88(5)	1.98(5)	2.858(4)	176(5)
Complex **6**					
N(2)–H(2N)···O(4)	$x, -y - 1/2, z + 1/2$	0.77(9)	2.24(10)	3.006(10)	173(9)
N(3)–H(3N)···O(2)	$x, -y - 1/2, z + 1/2$	0.87(9)	2.19(9)	3.039(10)	168(8)

and converge on a central pocket in which the nitrate anion is positioned in an fashion that is co-planar with the ligands, chelated between the two arms of the cationic complex. The structures are not, therefore, hydrogen-bonded polymers akin to the other species reported in this work, but instead are comprised of discrete entities, with the exception of hydrogen-bonded interactions to urea carbonyl moieties from ligated methanol in both cases. The $[Ag(\mathbf{1})_2]^+$ host system displays a remarkably good shape match for the nitrate anion.

Within the methanol solvate, **10**, the solvent is bound to the silver centre, resulting in a distorted trigonal geometry. The anion is not positioned symmetrically within the host complex, which would result in two $R_2^2(8)$ rings. Instead, the skewed orientation allows for a CH···O interaction to the nitrate, in addition to the four hydrogen bonds from the more acidic urea protons (Fig. 13). This off-centre position is a consistent feature of the four independent molecules in **10** and the three closely related independent molecules in **11**, although disorder is present in some complexes such that the nitrate can lie towards either the left- or right-hand side of the complex. The urea groups interact with the nitrate anion by means of both $R_2^2(8)$ and $R_1^2(6)$ motifs, as seen in the structure of **7**. The crystal packing of **10** is also remarkable, with 3.5 independent molecules contained in the asymmetric unit.[21] The half molecule displays an apparently linear Ag···O–N vector due to its position on a rotation axis, although this is merely a disorder average over two asymmetric orientations as adopted by the other three independent molecules. The long-range structure consists of discrete π-stacked heptamers held together by hydrogen bonding between the methanol and urea carbonyl (Fig. 14).

The MeOH/$MeNO_2$ solvate **11** also displays unusual crystal packing. The structure adopts the same space group as that of **10** ($C2/c$) but with two and a half independent molecules per

Table 3 Crystallographic data for complexes **7–11**

	7	**8**	**9**	**10**	**11**
Formula	$C_{27}H_{26.67}AgF_3N_6O_{5.33}S$	$C_{28}H_{31}AgN_7O_6F_3S$	$C_{52}H_{52}Ag_2N_{12}O_8S$	$C_{27}H_{30}AgN_7O_6$	$C_{27}H_{27.2}AgN_{7.6}O_{6.6}$
M	716.80	770.54	1220.86	656.45	671.63
Crystal system	Triclinic	Monoclinic	Tetragonal	Monoclinic	Monoclinic
Space group	P-1	$P2_1$	P-42_1c	$C2/c$	$C2/c$
a/Å	7.1774(5)	10.2326(11)	17.4146(6)	49.675(4)	30.599(3)
b/Å	16.7930(15)	15.6739(17)	17.4146(6)	13.4895(10)	13.8115(12)
c/Å	19.6054(18)	10.4685(11)	8.2655(6)	33.477(3)	32.625(3)
α/°	107.586(3)	90	90	90	90
β/°	93.998(3)	106.780(2)	90	122.132(7)	91.3120(10)
γ/°	91.066(4)	90	90	90	90
U/Å^3	2245.2(3)	1607.5(3)	2506.7(2)	18996(3)	13767(2)
Z	3	2	2	28	20
μ/mm^{-1}	0.810	0.763	0.892	0.799	0.792
Unique reflections	5223	7300	2878	20860	11431
Observed reflections	3996	6857	2766	18601	9242
R_{int}	0.0531	0.0351	0.0288	0.0613	0.0352
wR_2 (all data)	0.1419	0.0850	0.0706	0.2750	0.1261
R [$I \geq 2\sigma(I)$]	0.0566	0.0350	0.0288	0.0660	0.0519

Table 4 Hydrogen bond data for structures **7–11**

	Symmetry equivalent	*d*(D–H)/Å	*d*(H···A)/Å	*d*(D···A)/Å	∠(D–H···A)/°
Complex **7**[a]					
N(2)–H(2N)···O(5A)	$x+1, y+1, z$	0.88	1.91	2.72(4)	152.1
N(2)–H(2N)···O(5)	$x+1, y+1, z$	0.88	2.15	2.929(13)	147.8
N(3)–H(3N)···O(4)	$x+1, y+1, z$	0.88	2.19	3.043(16)	164.7
N(3)–H(3N)···O(5A)	$x+1, y+1, z$	0.88	2.20	2.97(4)	145.8
N(5)–H(5N)···O(4A)	x, y, z	0.88	2.10	2.96(3)	163.4
N(5)–H(5N)···O(6)	x, y, z	0.88	2.10	2.905(15)	151.5
N(6)–H(6N)···O(6)	x, y, z	0.88	1.98	2.783(12)	150.8
N(6)–H(6N)···O(6A)	x, y, z	0.88	2.13	2.95(3)	154.5
N(8)–H(8N)···O(7)	x, y, z	0.88	2.22	3.033(17)	153.9
N(8)–H(8N)···O(9)	$-x+2, -y, -z$	0.88	2.36	3.153(13)	150.7
N(9)–H(9N)···O(7)	x, y, z	0.88	2.04	2.881(16)	159.3
Complex **8**					
N(2)–H(2N)···O(5)	x, y, z	0.77(4)	2.48(4)	3.154(4)	146(4)
N(3)–H(3N)···O(5)	x, y, z	0.68(4)	2.19(4)	2.861(4)	175(5)
N(5)–H(5N)···O(7)	x, y, z	0.85(4)	2.11(4)	2.919(4)	160(4)
N(6)–H(6N)···O(7)	x, y, z	0.80(5)	2.23(5)	2.974(4)	156(4)
C(1)–H(1)···O(4)	x, y, z	0.93	2.97	3.715(4)	138.2
O(7)–H(2O)···O(4)	$x, y, z-1$	0.77(5)	2.14(5)	2.906(5)	171(4)
C(5)–H(5)···O(3)	$x, y, z-1$	0.93	2.78	3.591(4)	146.4
C(14)–H(14)···O(3)	$x, y, z-1$	0.93	2.45	3.296(4)	150.9
O(7)–H(1O)···O(1)	$x-1, y, z-1$	0.795(4)	2.049(4)	2.791(4)	155.3(4)
Complex **9**					
N(2)–H(2N)···O(2)	x, y, z	0.84(3)	2.18(3)	3.005(2)	168(3)
N(3)–H(3N)···O(2)	$-y+1, x, -z+1$	0.77(2)	2.08(3)	2.844(3)	174(2)
Complex **10**[ab]					
N(11)–H(11N)···O(106)	x, y, z	0.88	2.21	2.995(11)	148.0
N(12)–H(12N)···O(106)	x, y, z	0.88	2.16	2.922(9)	144.8
N(14)–H(14N)···O(107)	x, y, z	0.88	2.08	2.928(10)	162.1
N(15)–H(15N)···O(108)	x, y, z	0.88	2.06	2.940(9)	176.6
C(53)–H(53A)···O(107)	x, y, z	0.93	2.52	3.317(13)	142.0
Complex **11**[b]					
N(2)–H(2N)···O(7B)	x, y, z	0.83(6)	2.26(6)	3.02(2)	151(5)
N(3)–H(3N)···O(7B)	x, y, z	0.74(5)	2.16(6)	2.86(3)	158(6)
N(5)–H(5N)···O(6B)	x, y, z	0.73(4)	2.39(4)	3.084(9)	159(4)
N(6)–H(6N)···O(8B)	x, y, z	0.77(4)	2.15(5)	2.89(3)	162(4)
C(14)–H(14)···O(6B)	x, y, z	0.95	2.32	3.185(12)	150.4

[a] NH hydrogen positions are geometrically fixed. [b] Only data for one crystallographically independent $[Ag(\mathbf{1})_2]NO_3$ complex shown as an example for brevity.

asymmetric unit. Each asymmetric unit contains one $[Ag(\mathbf{1})_2]NO_3$ complex with nitromethane occupying the third coordination site, one complex with a 50 : 50 occupancy of nitromethane and methanol and the half complex is a methanol complex situated on the twofold rotation axis. As with **10** the nitrate anions are chelated by both urea groups in an offset fashion (with some disorder), allowing for CH···O as well as NH···O interactions. It is noteworthy that this discrete $ML_2(NO_3)$ unit persists with both MeOH and NO_2Me co-ligands. Moreover, the bidentate ligation of the Ag(I) centre by NO_2Me is highly unusual (Fig. 15), with only one previous example of this coordination mode to a transition metal, also silver(I), recorded in the CSD.[22]

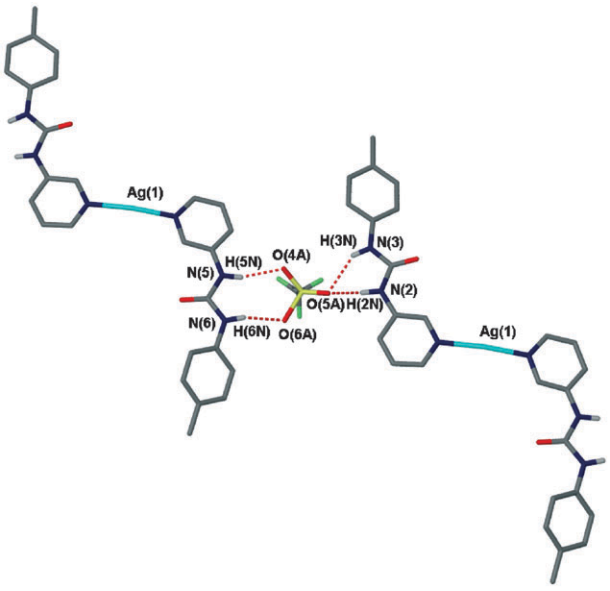

Fig. 8 The hydrogen bonding around one disordered triflate anion in **7**. Hydrogen bond data is given in Table 4.

Anion binding behaviour

The exact size and shape fit of the nitrate anion in the structures of **10** and **11** indicates that an assembly of this type may persist in solution. As a result we have undertaken a

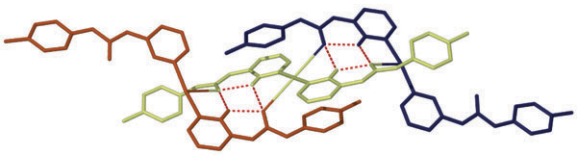

Fig. 9 A discrete trimeric assembly within the structure of **7** held together by long-range Ag–O interactions [2.851(5) and 2.967(6) Å] and weak CH···O interactions.

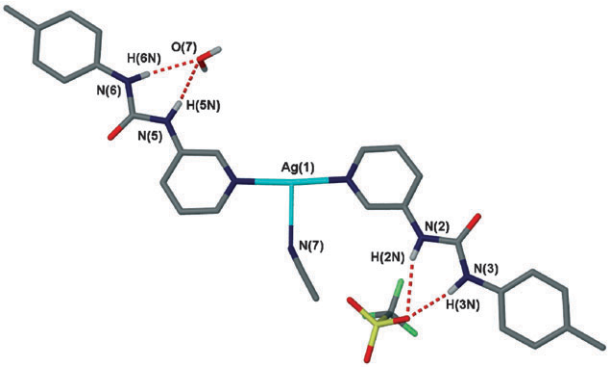

Fig. 10 The asymmetric unit of **8**, showing the urea groups in $R_1^2(6)$ interactions with both the triflate anion and water. CH hydrogen atoms not shown for clarity. Hydrogen bond data shown in Table 4.

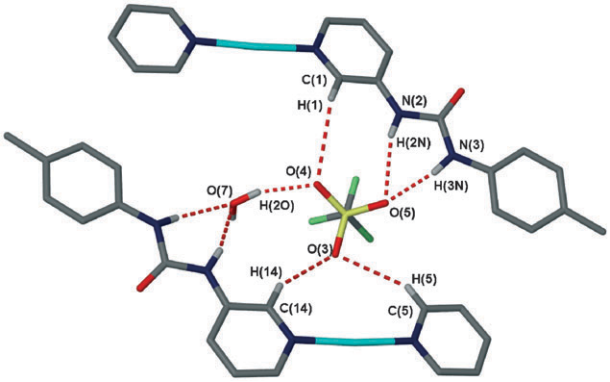

Fig. 11 The hydrogen bonding environment around the triflate anion in the structure of **8**. Coordinated acetonitrile omitted for clarity.

survey of the solution anion-binding properties of ligands **1** and **2** and their silver(I) complexes. The unbound ligands **1** and **2** themselves interact well with oxo-anions despite their lack of charge. ^{1}H NMR titrations were carried out in acetone on the uncoordinated ligands, with the oxo-anions added as tetrabutylammonium salts. Association constants were calculated for **1** and **2** using the program HypNMR[23] (Table 5).

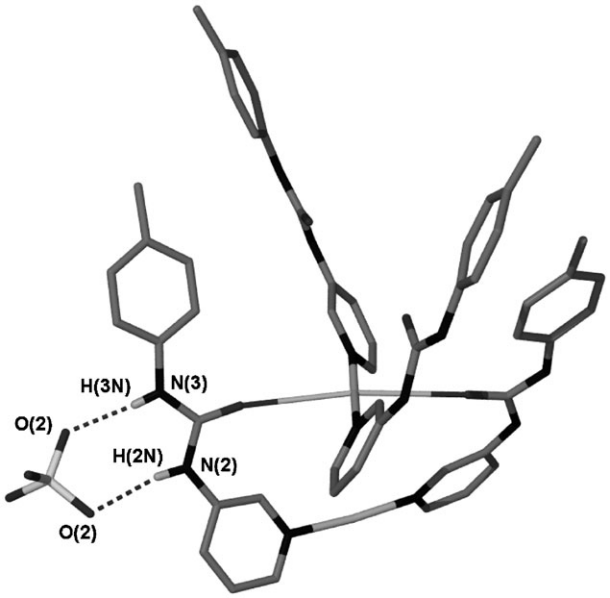

Fig. 12 Part of a helical chain in the structure of **9** held together by Ag–O interactions [Ag–O = 3.217(2) Å]. Hydrogen atoms omitted for clarity.

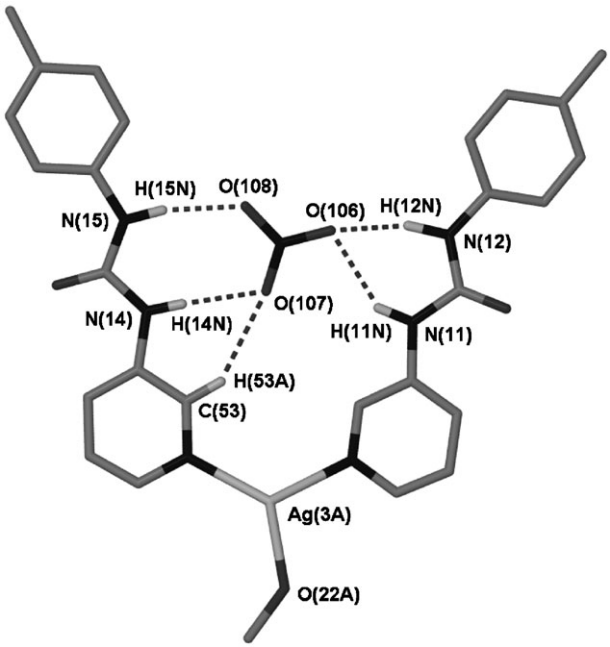

Fig. 13 Close size and shape complementarity of the nitrate anion with $[Ag(\mathbf{1})_2]^+$ in the structure of **10**.

These results show that nitrate and particularly acetate are both able to hydrogen bond strongly to the urea functionalities of the ligands. Upon addition of one equivalent of acetate to a solution of either **1** or **2** remarkable chemical shift changes of up to $\Delta\delta$ = 4.0 ppm are observed. Binding constants with this guest are above 10^5 M^{-1}, the limit of detection by NMR methods. This is attributable to the high basicity of the acetate anion. The spectra with acetate present also show a splitting of the urea NH proton signals into two species, believed to represent two separate binding modes, possibly with a dimeric structure forming, a phenomenon that is not observed for the binding of nitrate or perrhenate. Ligand **2** displays stronger anion binding than **1**, which may be due to the inductive effects of the pyridyl N atom on urea acidity.

The tweezer-like conformation of the $[Ag(\mathbf{1})_2]NO_3$ complex that exists in the solid-state structures of **10** and **11** is also observed to persist in solution. A ^{1}H NMR titration of $[Ag(\mathbf{1})_2]CF_3SO_3$ with nitrate (added as the tetrabutylammonium salt) clearly shows two separate binding events occurring when following the signal of the *para*-pyridyl proton (Fig. 16). Whilst the signals corresponding to the urea NH protons steadily move downfield during the experiment, the *para* pyridyl resonance displays a clear inflection point after the addition of one equivalent of nitrate, corresponding to a change in the binding mode. The first of these associations is believed to result in a 1 : 1 host–guest complex analogous to the solid-state structure with the subsequent binding event giving rise to a 1 : 2 stoichiometry. A Job plot confirms that this is indeed the case. The values of the association constants (K_{11} and K_{12}) are 30 200 and 2900 M^{-1} for the 1 : 1 and 1 : 2 complexes, respectively. In a preliminary communication we

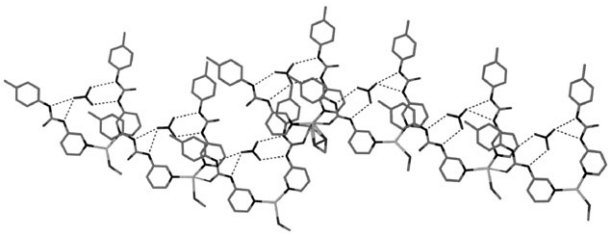

Fig. 14 A discrete heptameric assembly within the structure of **10**.

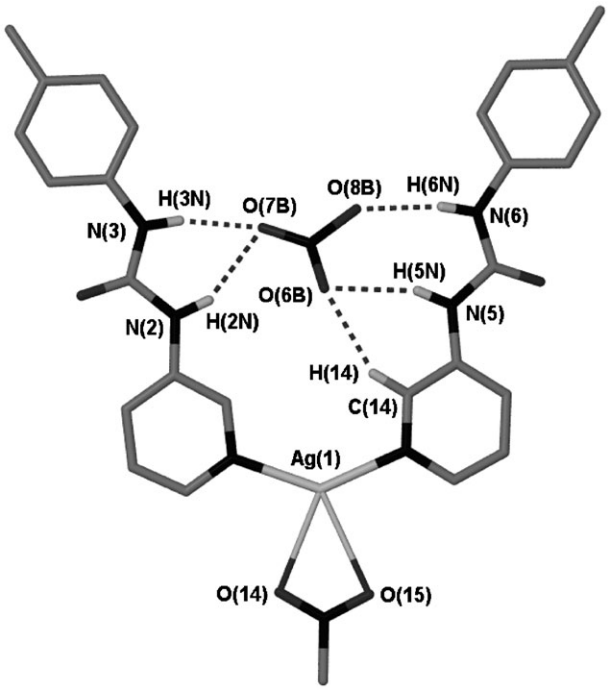

Fig. 15 The $[Ag(\mathbf{1})_2(MeNO_2)]NO_3$ complex within the structure of **11**. Selected bond lengths (Å): Ag(1)–O(14), 2.623(4); Ag(1)–O(15), 2.717(4). Only one disordered nitrate position shown.

reported slightly lower values.[11] The present data is of higher precision and was obtained at lower concentration, eliminating precipitation problems. In addition to these two binding constants that are associated with the urea ligands there is also a third, weaker binding process that is apparent during the modelling of the data (K_{13} = 550 M^{-1}). This is attributed to a direct coordination of the nitrate anion to the silver ion when a significant excess of the guest is present. Evidence for this process comes from the much stronger interaction of the metal centre with acetate (*vide infra*).

In the presence of the triflate anion there is apparently little or no chelation of the anion within the tweezer cavity, whereas the presence of the nitrate anion brings about a change in conformation, resulting in the chelated geometry observed in the crystal structure. This structure persists until addition of more than one equivalent of nitrate, at which point the chelated 1 : 1 structure gradually converts to a situation in which nitrate anions bind separately to the two ligands on the 'outside' of the complex in a fashion analogous to anion binding by free **1** (Fig. 17). Such a conformational change would significantly alter the environment of the *para*-pyridyl proton, with it facing towards the urea oxygen atom in the 1 : 1 complex and closer to a urea hydrogen atom in the 1 : 2 complex, giving rise to the observed change. The much higher value of K_{11} compared to K_{12} supports the formation of the chelated geometry observed crystallographically.

Titration of $[Ag(\mathbf{1})_2]CF_3SO_3$ with acetate produced a notably different response to that of nitrate. Very little change in the chemical shift values of the NH protons was observed until after the addition of one equivalent of acetate. This behaviour is attributed to the ligation of the Ag(I) centre by the first equivalent of acetate, unlike nitrate, which does not ligate until an excess of the guest is present (Fig. 18). The addition of further aliquots of TBA-acetate produced significant binding, although there was no evidence of two separate binding events as observed for nitrate. Hence, the behaviour of the complex was modelled as 1 : 1 and 1 : 3 aggregates, with values of K_{11} and $K_{12} \times K_{13}$ found to be 4.97×10^5 and 5.31×10^6 M^{-1}, respectively. It is speculated that either a complex in which one acetate anion binds to each arm forms, or, the ligation of the acetate causes a break-up of the $[Ag(\mathbf{1})_2]^+$ complex and the arms act independently. The acetate anion is not of the correct shape to template the formation of the tweezer geometry of the complex and therefore a very different conformation may result.

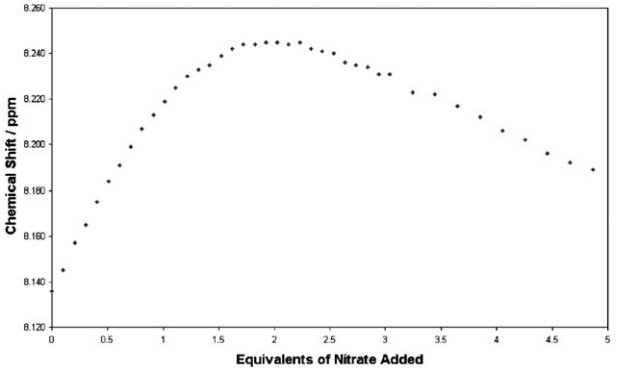

Fig. 16 The chemical shift change of the *para*-pyridyl proton during the titration of $[Ag(\mathbf{1})_2]CF_3SO_3$ + TBA-NO_3, showing two different processes occurring.

Binding of perrhenate by $[Ag(\mathbf{1})_2]^+$ was almost negligible, as expected for this labile anion with diffuse charge. An upfield shift is observed for the urea proton signals, contrary to the downfield shifts observed for acetate and nitrate. This suggests that the perrhenate anion is hydrogen bonded less strongly than the triflate anion that it displaces.

Unfortunately, the solution behaviour of the $[Ag(\mathbf{2})_2]^+$ complex could not be ascertained due to its insolubility. However, this complex is not expected to show cooperative binding between the ligands due to the position of the urea group on the pyridyl ring, as evidenced in the crystal structures obtained.

Conclusions

The complexes obtained with various anions using both the $[Ag(\mathbf{1})_2]^+$ and $[Ag(\mathbf{2})_2]^+$ cations show that the urea functionality has a strong tendency to form $R_2^2(8)$ motifs with oxoanions. When this affinity is harnessed into a host assembly with the correct geometry for a specific guest, as in the case of $[Ag(\mathbf{1})_2]NO_3$, then significant binding persists in solution with the binding of the templating anion markedly enhanced

Table 5 Binding constants (M^{-1}) obtained *via* ^{1}H NMR titrations for the free ligands **1** and **2** and the complex $[Ag(\mathbf{1})_2]^+$

	1	**2**	$[Ag(\mathbf{1})_2]^+$		
Anion	K_{11}	K_{11}	K_{11}	K_{12}	K_{13}
NO_3^-	956	3500	30 200[c]	2900	550[c]
$CH_3O_2^-$	$>10^5$ [a]	$>10^5$ [a]	4.97×10^5 [c]	— [b]	5.31×10^6 [cd]
ReO_4^-	$<10^a$	$<10^a$	$<10^a$	$<10^a$	$<10^a$

[a] Binding constants are too high/low to be accurately determined. [b] Acetate does not form an identifiable 1 : 2 complex with $[Ag(\mathbf{1})_2]^+$, see text. [c] For nitrate K_{13} represents the ligation of the anion to the metal centre, whereas for acetate K_{11} represents this process, see text. [d] Modelled as simultaneous binding of two anions, *i.e.*, $K_{12} \times K_{13}$.

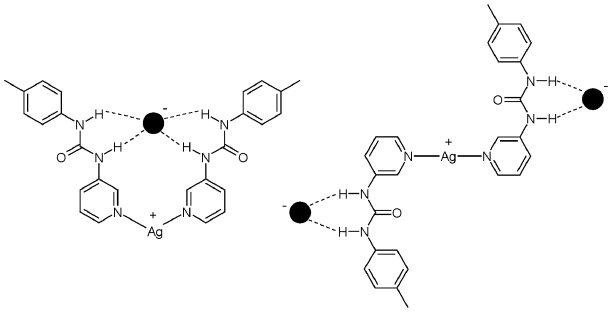

Fig. 17 The two proposed conformations adopted by the $[Ag(\mathbf{1})_2]^+$ host in solution with either one anion coordinated between arms or with the arms binding independently.

compared to the free ligand. In the presence of strongly ligating anions such as acetate, however, the self-assembly process is disrupted by direct binding of the anion to the metal centre.

Experimental

The syntheses of the ligands **1** and **2** have previously been reported.[12] All commercial starting materials and solvents were used as purchased with no further purification or drying. The syntheses of **3–11** were aimed toward the formation of crystalline samples and generally proceeded in good yield. Elemental analyses were carried out at the University of Durham using an Exeter Analytical E-440 instrument.

^{1}H NMR titration experiments were conducted in acetone-d_6 using a Varian Mercury 400-BB spectrometer with TMS as an internal reference. An initial concentration of 0.034 mol dm^{-3} of **1** or **2** was used in all cases, with the guest anions added as tetrabutylammonium salts in 10 μl aliquots (corresponding to 0.1 equivalents of the guest).

Synthesis

$[Ag(2)_2]CF_3SO_3 \cdot 2H_2O$ (3). Crystals grown from a solution of **2** (0.050 g, 0.22 mmol) and $AgCF_3SO_3$ (0.057 g, 0.22 mmol) in water–methanol (50 : 50 v/v; 5 ml) at room temperature. Anal. calcd for $C_{27}H_{30}N_6O_7SF_3Ag$: C, 43.38; H, 4.05; N, 11.24%; found: C, 43.36; H, 4.05; N, 11.27%.

$[Ag(2)_2]CH_3CO_2 \cdot 1.25H_2O \cdot MeOH$ (4). Crystals grown from a solution of **2** (0.050 g, 0.22 mmol) and $AgCH_3CO_2$ (0.037 g, 0.22 mmol) in water–methanol (50 : 50 v/v; 5 ml) at room temperature. Anal. calcd for $C_{29}H_{34.5}N_6O_{6.25}Ag$: C, 51.53; H, 5.26; N, 12.44%; found: C, 51.55; H, 5.27; N, 12.52%.

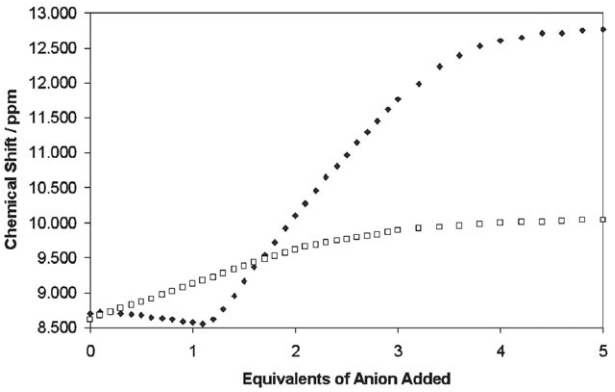

Fig. 18 Titration plots of $[Ag(\mathbf{1})_2]CF_3SO_3$ with TBA-NO_3 (squares) and TBA-CH_3CO_2 (diamonds) following the urea NH resonance adjacent to the pyridyl ring. The first equivalent of acetate coordinates to the silver before binding occurs with increasing guest concentration, whereas with nitrate binding occurs prior to coordination.

$[Ag(2)_2]NO_3 \cdot H_2O$ (5). Crystals grown from a solution of **2** (0.050 g, 0.22 mmol) and $AgNO_3$ (0.038 g, 0.22 mmol) in wet acetonitrile (5 ml) at room temperature. Anal. calcd for $C_{26}H_{30}N_7O_6Ag$: C, 48.61; H, 4.39; N, 15.26%; found: C, 48.35; H, 4.37; N, 15.32%.

$[Ag(2)]NO_3$ (6). Crystals grown from a solution of **2** (0.050 g, 0.22 mmol) and $AgNO_3$ (0.038 g, 0.22 mmol) in methanol (5 ml) at room temperature. Anal. calcd for $C_{13}H_{13}N_4O_4Ag$: C, 39.32; H, 3.30; N, 14.11%; found: C, 39.25; H, 3.28; N, 14.16%.

$[Ag(1)_2]CF_3SO_3 \cdot 0.5H_2O$ (7). Crystals grown from a solution of **1** (0.025 g, 0.11 mmol) and $AgCF_3SO_3$ (0.0094 g, 0.04 mmol) in cyclohexane–methanol (50 : 50 v/v; 5 ml) at room temperature. Anal. calcd for $C_{27}H_{27}N_6O_{5.5}SF_3Ag$: C, 45.00; H, 3.75; N, 11.67%; found: C, 45.23; H, 3.77; N, 11.60%.

$[Ag(1)_2]CF_3SO_3 \cdot H_2O \cdot MeCN$ (8). Crystals grown from a solution of **1** (0.025 g, 0.11 mmol) and $AgCF_3SO_3$ (0.0094 g, 0.04 mmol) in water–acetonitrile (50 : 50 v/v; 5 ml) at room temperature. Anal. calcd for $C_{29}H_{31}N_7O_6SF_3Ag$: C, 45.19; H, 4.02; N, 12.73%; found: C, 45.26; H, 4.12; N, 12.62%.

$[Ag(1)_2]_2SO_4$ (9). Crystals grown from a solution of **1** (0.025 g, 0.11 mmol) and $AgSO_4$ (0.011 g, 0.04 mmol) in acetonitrile–water (50 : 50 v/v; 5 ml) at room temperature. Anal. calcd for $C_{52}H_{52}N_{12}O_8Ag_2S$: C, 51.15; H, 4.26; N, 13.77%; found: C, 51.01; H, 4.21; N, 13.83%.

$[Ag(1)_2]NO_3 \cdot MeOH$ (10). Crystals grown from a solution of **1** (0.025 g, 0.11 mmol) and $AgNO_3$ (0.006 g, 0.04 mmol) in toluene–methanol (50 : 50 v/v; 5 ml) at room temperature. Anal. calcd for $C_{27}H_{30}N_7O_6Ag$: C, 49.39; H, 4.57; N, 14.94%; found: C, 48.93; H, 4.27; N, 15.16%.

$[Ag(1)_2]NO_3 \cdot 0.4MeOH \cdot 0.6MeNO_2$ (11). Crystals grown from a solution of **1** (0.025 g, 0.11 mmol) and $AgNO_3$ (0.006 g, 0.04 mmol) in nitromethane–methanol (50 : 50 v/v; 5 ml) at 4 °C. Anal. calcd for $C_{27}H_{29.5}N_{7.5}O_{6.5}Ag$: C, 48.32; H, 4.40; N, 15.66%; found: C, 48.05; H, 4.43; N, 15.48%.

Crystallography†

X-Ray diffraction data were collected using either Bruker 3-circle diffractometers with SMART 1000 (**3–6**, **10**) or Apex (**8**, **9** and **11**) CCD detectors or a Nonius KappaCCD diffractometer (**7**), with monochromated Mo-Kα radiation in all cases. All data were collected at 120 K as maintained by Oxford Cryosystems open-flow N_2 cryostats. The structures were solved by direct methods using SHELXS-97[24] and refined by full-matrix least squares against F^2 of all reflections using SHELXL-97.[25] All C–H bond lengths were set to fixed X-ray distances, as were N–H bonds in lower quality data sets (0.880 Å), and allowed to ride. Hydrogen atoms attached to oxygen or nitrogen were located experimentally from difference Fourier maps, except in the cases of **7** and **10** for which the data quality was not sufficient to permit this. All hydrogen atoms are treated with isotropic atomic displacement parameters.

Structure **7** contains one triflate anion that has an SO_3 group disordered over two positions (50 : 50 occupancies) between two urea groups. The half triflate per asymmetic unit exists in the same site as the half occupancy enclathrated water molecule, refined as separate parts. Structure **10** contains disordered

† CCDC reference numbers are 256159–256167 for **3**–**11**. See http://www.rsc.org/suppdata/nj/b4/b415818k/ for crystallographic data in .cif or other electronic format.

methanol ligands on two of the independent molecules. Structure **11** contains disordered nitrate anions (two and a half per asymmetric unit) across two positions, centred around the nitrogen atom, of 50 : 50 occupancies.

Acknowledgements

We thank the EPSRC for studentships (DRT, ECS) and for an advanced fellowship (JAKH). Special thanks to Dr Len Barbour, University of Stellenbosch, South Africa, for the SHELX [25] interface program X-Seed (www.x-seed.net).[26]

References

1 P. A. Gale, *Coord. Chem. Rev*., 2003, **240**, 191.
2 P. A. Gale, *Coord. Chem. Rev*., 2001, **213**, 79.
3 F. P. Schmidtchen and M. Berger, *Chem. Rev*., 1997, **97**, 1609.
4 T. S. Snowden and E. V. Anslyn, *Curr. Opin. Chem. Biol*., 1999, **6**, 740.
5 C. F. Mason, *Biology of Freshwater Pollution*, Longman, Harlow, Essex, 2nd edn., 1991.
6 K. J. Wallace, R. Daari, W. J. Belcher, L. Abouderbala, M. G. Boutelle and J. W. Steed, *J. Organomet. Chem*., 2003, **666**, 63.
7 X. L. Chi, A. J. Guerin, R. A. Haycock, C. A. Hunter and L. D. Sarson, *J. Chem. Soc., Chem. Commun*., 1995, 2563.
8 C. R. Bondy and S. J. Loeb, *Coord. Chem. Rev*., 2003, **240**, 77.
9 C. R. Bondy, P. A. Gale and S. J. Loeb, *Chem. Commun*., 2001, 729.
10 C. R. Bondy, P. A. Gale and S. J. Loeb, *J. Am. Chem. Soc*, 2004, **126**, 5030.
11 D. R. Turner, E. C. Spencer, J. A. K. Howard, D. A. Tocher and J. W. Steed, *Chem. Commun*., 2004, 1352.
12 D. R. Turner, B. Smith, A. E. Goeta, I. Radosavljevic-Evans, D. A. Tocher, J. A. K. Howard and J. W. Steed, *CrystEngComm*, 2004, submitted.
13 D. R. Turner, M. B. Hursthouse, M. E. Light and J. W. Steed, *Chem. Commun*., 2004, 1354.
14 M. Albrecht, J. Zauner, R. Burget, H. Rottele and R. Frohlich, *Mater. Sci. Eng. C*, 2001, **18**, 185.
15 J. Bernstein, R. E. Davis, L. Shimoni and N.-L. Chang, *Angew. Chem., Int. Ed. Engl*., 1995, **33**, 143.
16 (*a*) *CSD Version 5.25*, CCDC, Cambridge, Nov. 2003; (*b*) F. H. Allen, *Acta Crystallogr., Sect. B*, 2002, **58**, 380.
17 M. C. Etter, *Acc. Chem. Res*., 1990, **23**, 120.
18 F. A. Cotton, G. Wilkinson, C. A. Murillo and M. Bochman, *Advanced Inorganic Chemistry*, John Wiley and Sons, New York, 1999.
19 S. C. Blackstock and J. K. Kochi, *J. Am. Chem. Soc*., 1987, **109**, 2484.
20 Y. A. Simonov, M. D. Mazus, S. T. Malinovsky, E. S. Levchenko, S. V. Pavlova and L. I. Budarin, *Kristallografiya*, 1987, **32**, 93.
21 J. W. Steed, *CrystEngComm*, 2003, 169.
22 N. Schulthiess, D. R. Powell and E. Bosch, *Inorg. Chem*., 2003, **42**, 8886.
23 P. Gans, *HypNMR*, Protonic Software, University of Leeds, Leeds, 2000.
24 G. M. Sheldrick, *SHELXS-97, Program for solution of crystal structures*, University of Göttingen, Germany, 1997.
25 G. M. Sheldrick, *SHELXL-97, Program for refinement of crystal structures*, University of Göttingen, Germany, 1997.
26 L. J. Barbour, *J. Supramol. Chem*., 2001, **1**, 189.